International Journal of Thermophysics, Vol. 26, No. 6, November 2005 (© 2005)
DOI: 10.1007/s10765-005-8586-3

A Microwave–Ultrasonic Cell for Sound-Speed Measurements in Liquids[1]

G. Benedetto,[2] R. M. Gavioso,[2] P. A. Giuliano Albo,[2] S. Lago,[2] D. Madonna Ripa,[2,3] and R. Spagnolo[2]

In this work preliminary results obtained in developing a prototype cylindrical ultrasonic cell designed to apply a microwave resonance technique to the determination of its internal dimensions are described. Since the apparatus is intended for speed-of-sound measurements in pressurized liquid-phase media, the cell design is such that a double reflector pulse-echo technique can be used for time-of-flight measurements. The main absorption and dispersion effects that influence the acoustic measurement in this interferometer-like configuration and the values of the corresponding corrections are considered and discussed. The performance of the experimental apparatus and method in terms of achievable precision and accuracy was tested by measuring the speed of sound in water on a single isotherm at 325 K between 0.1 and 90 MPa.

KEY WORDS: microwave resonator; pulse-echo method; speed of sound.

1. INTRODUCTION

Any sound-speed measurement apparatus needs an independent procedure to evaluate some geometric features of the system, directly or indirectly, related to the physical path length traveled by the sound wave. In steady-state techniques, these are the characteristic dimensions of a resonant cavity of simple geometry, in transient techniques, the distance between a pulse source and a reflector. While high accuracy and precision can easily be achieved in time or frequency measurements, the determination

[1] Paper presented at the Fifteenth Symposium on Thermophysical Properties, June 22–27, 2003, Boulder, Colorado, U.S.A.

[2] Istituto Elettrotecnico Nazionale Galileo Ferraris, Strada delle Cacce 91, I-10135 Torino, Italy.

[3] To whom correspondence should be addressed. E-mail: mripa@ien.it

of the actual geometric path length appears to be the main limiting factor when attempting to reduce the uncertainty budget of a speed-of-sound measurement.

In this work, we describe a prototype ultrasonic cell consisting of a plane piezoelectric (PZT) transducer, stainless steel reflectors, and spacers which form a double cylindrical conducting cavity. The transducer –reflector distances are calculated determining the length of the two cavities from measurements under vacuum of microwave resonances of a few transverse electric (TE) and transverse magnetic (TM) modes of different symmetry. Corrections are then applied on the basis of the coefficient of compressibility of stainless steel to take into account the pressure dependence of the calculated path-length difference.

In the acoustic configuration, the cell is designed to determine the difference in the propagation time of an acoustic pulse between the PZT transducer and the opposite reflectors, realizing a traditional double pulse-echo method [1, 2]. As the acoustic source and the propagating cavity have the same cross section, the acoustic propagation is very much like that taking place in an interferometer. The correction due to the absorption effect from the walls of the two cavities is on the order of a few ppm, a negligible additional contribution to the overall uncertainty. An upper limit to the influence of dispersion and diffraction effects was assessed to be on the order of 20 ppm on the basis of theoretical models from different sources.

As a first test of the performance of the method, pulse-echo measurements were performed at 325 K between atmospheric pressure and 90 MPa on a sample of high purity water, using results of dimensional measurements obtained at the same temperature from the microwave resonances of the TE111 and TE112 modes of the two cylindrical cavities. The determined speed-of-sound data have been compared with the predictions of the IAPWS-95 formulation [3] with an observed deviation of 0.05%.

2. MICROWAVE MEASUREMENTS

2.1. Experimental Apparatus

The prototype microwave-ultrasonic cell used in this work is shown in Fig. 1. It consists of two AISI 303 stainless steel cylindrical cavities having an outer diameter of 60 mm, an internal diameter of 42 mm, and lengths of 40 and 60 mm. Two solid stainless steel reflectors (4 mm thick) are fixed to the ends of the cell to form two geometrically regular cylindrical conducting cavities separated by a piezoelectric disc having a diameter of 45 mm and a thickness of 0.25 mm.

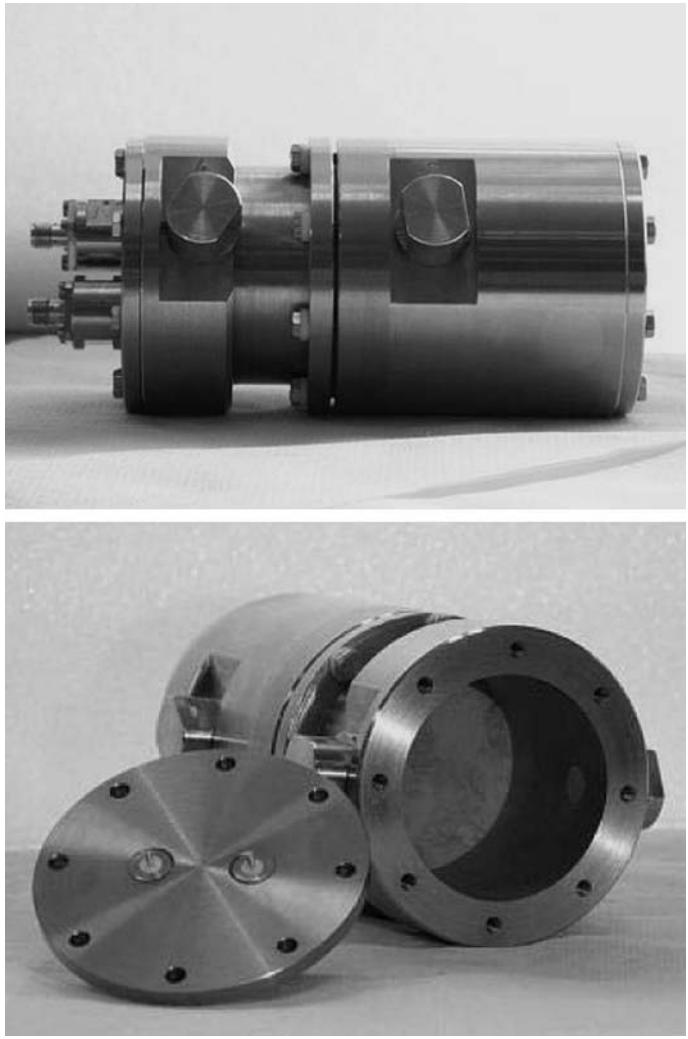

Fig. 1. Photograph of the double cylindrical cavity used in this work for microwave and pulse-echo measurements.

The disc is pressed between the mating surfaces of the cavities and fixed by eight (M3) screws and bolts. Two threaded holes were located on the sidewall of the two cavities and served either for filling and evacuation of the cell with the liquid under test or for mounting two probes made up of a straight, gold-plated copper conductor which protruded 3 mm into the

cylindrical cavity. During the microwave measurements, the cell was placed inside a vacuum-tight vessel within a thermostatted bath. The temperature of the cell was measured with a platinum resistance thermometer. Semi-rigid coaxial cables led from each probe via feedthroughs to a network analyzer (Agilent 8719ES) which permitted measurements up to 13.5 GHz.

The instrumentation, materials, and procedures used in the acoustic configuration are described elsewhere [4].

2.2. Theory of Microwave Resonances in a Cylindrical Cavity

The experimental techniques based on the analysis of the frequency spectrum of cylindrical conducting cavities for a determination of their internal dimensions are well-established and have been used for many different applications [5, 6]. Recently, a small dimension brass cylindrical cavity has been realized for measurements of the relative permittivity of gases [6].

The normal modes in a right circular cylinder of diameter D and length L can be divided in TE- and TM-classes where the axis of reference z is along the cylinder axis. These modes are further specified in terms of three integers m, n, and p, which are defined as the number of full-period variations of the different components of the electromagnetic field with respect to the angular, radial, and longitudinal coordinates. The normal mode fields are expressed in terms of the trigonometric and Bessel functions, and the corresponding resonance frequencies, for the case of a cavity with perfectly conducting walls, are given by the equation,

$$f_{mnp}^2 = \left(\frac{c}{2\pi\sqrt{\mu\varepsilon}}\right)^2 \left(\frac{4\chi_{m,n}^2}{D^2} + \frac{\pi^2 p^2}{L^2}\right) \tag{1}$$

where c, μ, and ε are, respectively, the speed of light, the magnetic permeability, and the dielectric constant of the medium which fills the cavity, $\chi_{m,n}$ is the nth root of $J_m(x) = 0$ for TM-modes ($m, p = 0, 1, 2, \ldots ; n = 1, 2, \ldots$), or the nth root of $J'_m(x) = 0 (m = 0, 1, 2, \ldots ; n, p = 1, 2, \ldots)$ for TE-modes, and $J_m(x)$ is the cylindrical Bessel function of order m. According to Eq. (1) and to the selection rules reported above, the frequencies of the TM$mn0$ modes depend only on the cavity diameter D and not on its length L. All the other modes have resonance frequencies which depend both on D and L, so that a minimum of two modes is necessary for the determination of the length of a cylindrical cavity. However, it should be noted that, from a metrological point of view, the most appropriate choice for this purpose contemplates two *related* modes which differ

only for the value of the index p, having equal values of the indexes m and n.

This being the case, we can consider the following system:

$$\begin{cases} f_{mnp_1}^2 = \left(\frac{c}{2\pi\sqrt{\mu\varepsilon}}\right)^2 \left(\frac{4\chi_{m,n}^2}{D^2} + \frac{\pi^2 p_1^2}{L^2}\right) & \text{(2a)} \\ f_{mnp_2}^2 = \left(\frac{c}{2\pi\sqrt{\mu\varepsilon}}\right)^2 \left(\frac{4\chi_{m,n}^2}{D^2} + \frac{\pi^2 p_2^2}{L^2}\right) & \text{(2b)} \end{cases}$$

from which we obtain

$$L^2 = \frac{c^2\left(p_2^2 - p_1^2\right)}{4}\left(f_{mnp_2}^2 - f_{mnp_1}^2\right)^{-1}. \quad (3)$$

As implied by the absence of D and by the dependence of L^2 on $f_{mnp_{1,2}}^2$ in Eq. (3), it is evident that possible systematic errors associated with the determination of the resonance frequencies of a couple of *related* modes would not affect the determination of L to a first order of approximation. Thus, apart from random errors associated with their measurement, the resonance frequencies of a couple of *related* modes are determined by exactly the same diameter and very nearly by the same length. As evidenced in Fig. 2, which shows the low frequency microwave spectrum of the two cavities which comprise the ultrasonic cell, the relative separation and position of modes of different symmetry depend on the value of the ratio D/L.

The reported spectra were recorded by the two antennae mounted on the sidewall of the two cavities. This position does not allow excitation of the TM$mn0$ modes, whose frequency depends only on the cavity diameter, and are of no interest for a determination of its length. The probes could also be alternatively mounted on the reflectors which form the basis of the cylindrical cavities; this position however did not allow detection of the whole class of the TEmnp modes. Positioning the antennae on the sidewall of the cavity then revealed two major advantages: (i) inefficient detection of TM$mn0$ modes results in a better separation of low-frequency modes of different symmetry; and (ii) removal of the antennae from their ports for the acoustic measurements was possible without replacing or dismounting the reflectors, allowing a better reproducibility of the lengths alternatively sensed by the acoustic pulses and the microwave field. The results illustrated throughout the rest of this work were obtained with this configuration of the microwave probes. A casual inspection of Fig. 2 shows that, according to the discussion above, the TE111 and TE112 modes are the best candidates for a determination of the lengths L_1 and L_2 of the two cavities, because of their good isolation from other neighboring modes.

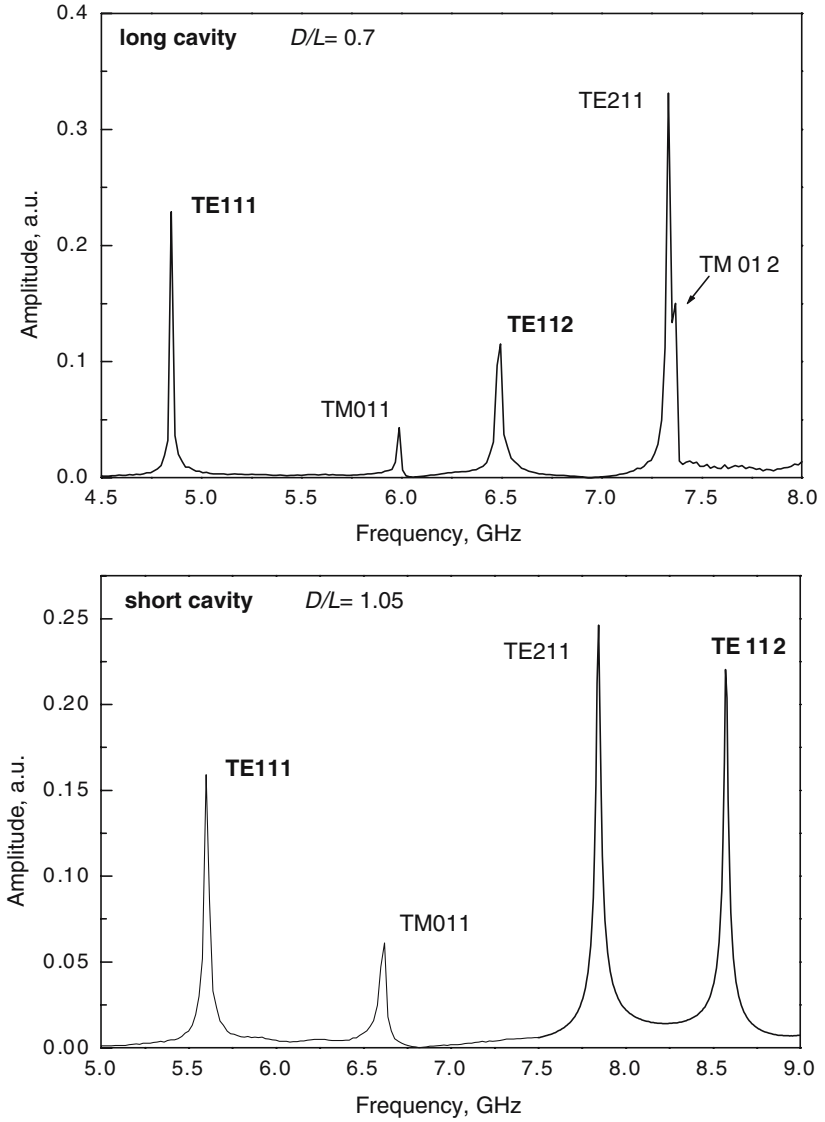

Fig. 2. Microwave spectrum of the two cylindrical cavities constituting the ultrasonic cell: Top: long cavity $D/L = 0.70$; Bottom: short cavity $D/L = 1.05$.

2.3. Data Acquisition

Typically 101 frequencies spanning each mode under study were recorded as the average of 10 scans with an intermediate-frequency (IF) bandwidth of 10 Hz. The network analyzer was configured to measure the four scattering coefficients $\mathbf{S}_{ij}$; however, only the coefficient $\mathbf{S}_{12}$ was utilized for the succeeding data analysis. The averaged real and imaginary parts of the signal were fitted to a complex Lorentzian function of the frequency [7].

As an example of the extremely high level of precision of the fitting procedure and consequently of the resonance frequencies determination, Fig. 3 reports the results obtained in fitting the TE111 mode for the long cavity.

2.4. Widths of Microwave Resonances

When the wall of the cavity has a finite conductivity σ, the exponential decay of the electromagnetic field within the wall results in a contribution to the half-widths of the resonances and in an equal reduction of the frequencies. The magnitude of these effects is for TM- and TE-modes, respectively [8],

$$\frac{\Delta f_N + \mathrm{i} g_N}{f_N} = (-1+\mathrm{i}) \cdot \delta \cdot \left(\frac{1}{D} + \frac{1}{L} \right) \tag{4a}$$

$$\frac{\Delta f_N + \mathrm{i} g_N}{f_N} = (-1+\mathrm{i}) \cdot \delta \cdot \left(\frac{\chi_{mn}^2}{D\left(\chi_{mn}^2 - m^2\right)} + \frac{1}{L} - \frac{(\pi p)^2 D + 4\chi_{mn}^2 L}{(\pi p)^2 D + 4\chi_{mn}^2 L^2} \right) \tag{4b}$$

where N summarizes the set of three indexes (nmp), $\boldsymbol{F}_N = f_N + i g_N$ is the complex resonance frequency of the mode under study (with g_N representing the half-width of the resonance curve which is determined by the various energy losses present in the system), and δ is the penetration length given by

$$\delta = (\pi f_N \mu \sigma)^{-0.5}. \tag{5}$$

In order to calculate g_N for the modes of interest, we assumed $\mu = \mu_0$, the permeability of free space, and we estimated the conductivity at 325 K as an average of the dc data reported in Ref. 9 for a variety of different stainless steel samples.

2.5. Microwave Results

We made measurements in the proximity of the modes TE111, TM011, and TE112 on a single isotherm near 325 K for the two cylindrical cavities comprising the ultrasonic cell. The results are reported in Table I, where

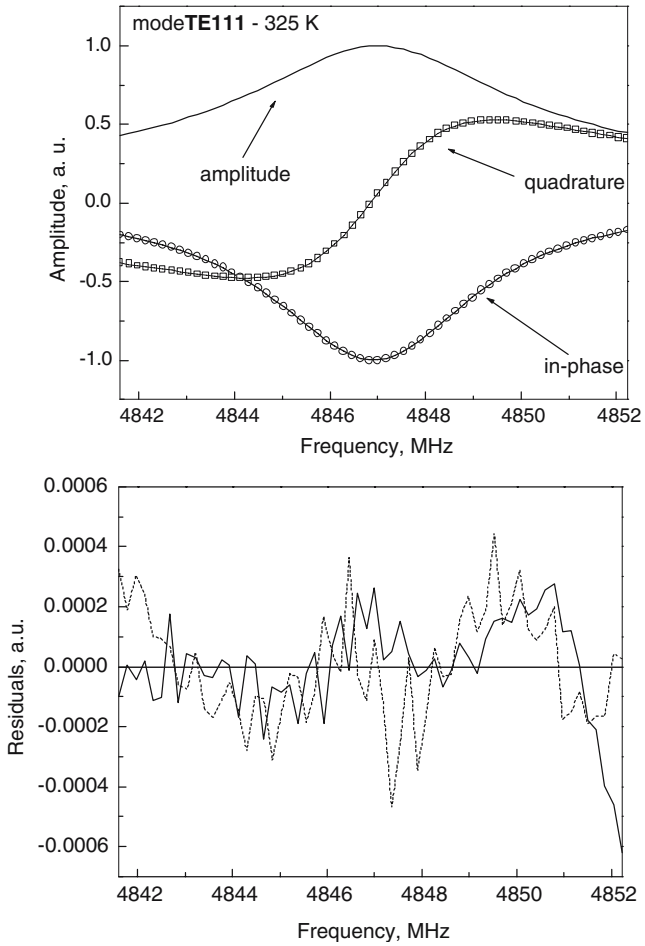

Fig. 3. Top: In-phase and quadrature signals detected by the network analyzer in correspondence of the TE111 mode in the longer cavity. Bottom: deviations of the detected signal from a fit with a complex Lorentzian function to the experimental data.

are listed: the experimental values of the resonance frequency $f_N(\text{exp})$ and half-width $g_N(\text{exp})$; the corresponding standard deviation $\sigma(\text{fit})$ expressed as a fraction of the maximum measured amplitude; the calculated value of the half-width $g_N(\text{calc})$ determined with Eq. (4a,b) and the resistivity data in Ref. 9; the difference between experimental and calculated half-widths scaled by the value of the resonance frequency $\Delta g_N/f_N$, and the estimated relative random uncertainty associated with the frequency measurement

Table I. Results of Microwave Measurements

Mode	f_N(exp) (GHz)	g_N(exp) (MHz)	g_N(calc) (MHz)	$\Delta g_N/f_N$	σ(fit)	$(\sigma f_N/f_N)$
Short cavity $(D/L=1.05)$ at $T=325.06$ K						
TE111	5.600884	4.628	1.156	6.2×10^{-4}	2.7×10^{-4}	2.7×10^{-7}
TE112	8.573530	11.11	1.448	1.1×10^{-3}	1.2×10^{-3}	3.1×10^{-6}
TM011	6.610024	5.215	1.788	5.2×10^{-4}	3.4×10^{-4}	5.4×10^{-7}
Long cavity $(D/L=0.70)$ at $T=325.06$ K						
TE111	4.846975	2.583	0.997	3.3×10^{-4}	3.7×10^{-4}	3.9×10^{-7}
TE112	6.483638	3.840	1.070	4.3×10^{-4}	2.0×10^{-4}	2.4×10^{-7}
TM011	5.983583	3.159	1.406	2.9×10^{-4}	2.0×10^{-4}	1.9×10^{-7}

$(\sigma f_N/f_N)$ calculated as $2(g_N/f_N)\sigma$(fit). When the isotherm at 325 K was completed and the results examined, it became evident, as shown from the data reported in Table I, that a substantial disagreement existed between the experimental and calculated half-widths for all the modes under study. A calculation of the expected resonance frequencies for the two cavities, made on the basis of their nominal dimensions at ambient temperature and the coefficient of thermal expansion, indicated a systematic difference of similar magnitude. Following these observations we suspected the existence of a problem of overcoupling between the resonant cavity and the straight probe antennae used to excite and detect the microwave resonances. In order to test this hypothesis, we removed the microwave probe in the short cavity and replaced it with a stainless steel plug whose front surface was machined to be flush with the interior surface of the cavity and reproduced its curvature. We configured the network analyzer to measure the reflection coefficient $\mathbf{S}_{11}$ on a large frequency interval spanning the resonance curve of the mode TE112, and compared the results with those obtained with the two microwave probes and transmission lines connected to the cavity. This comparison, which is illustrated in Fig. 4, revealed a substantial decrease of the width of the resonance curve and a corresponding increase in the resonance frequency confirming the hypothesis discussed above.

Although aware of this possible source of systematic error, we used the experimental half-widths to correct the experimental frequencies of the modes TE111 and TE112 at 325 K for the two cavities and calculated the distances L_1 and L_2 between the transducer and the two reflectors by use of Eq. (3) and finally obtained the difference ΔL at zero pressure. The relative uncertainty associated to the present determination of ΔL was estimated to be on the order of 5×10^{-4}, which corresponds to the observed

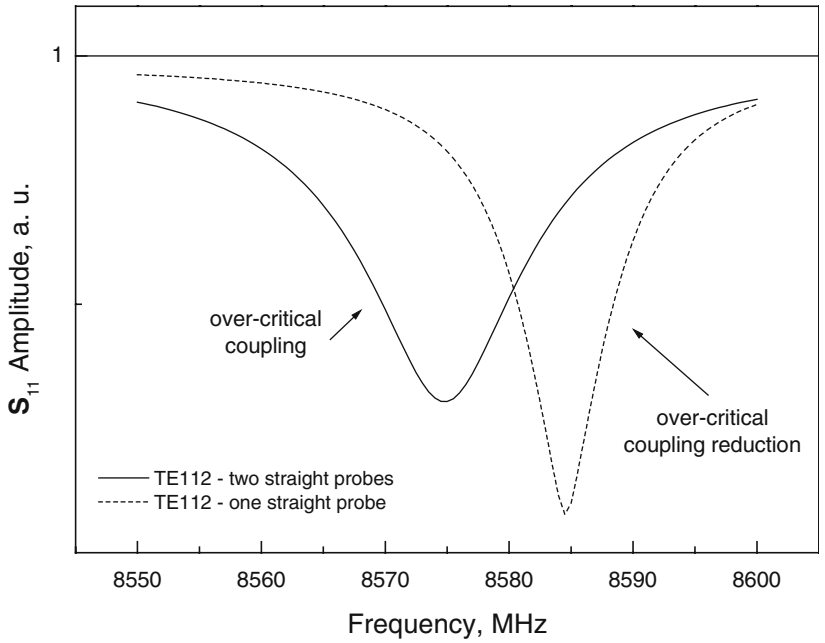

Fig. 4. Evidence of an overcoupling effect on microwave resonances.

average deviation between measured and calculated half-widths of the TE modes used for this purpose.

3. ACOUSTIC MEASUREMENTS

The double cavity cell design is the result of a compromise between the necessity of limited overall dimensions, which permit the insertion of the cell in our high pressure vessel, and the limited bandwidth of the network analyzer. Because our aim was to check the feasibility of a high precision geometrical path determination, the ultrasonic cell design is not, in any way, the state of the art in the field of acoustic sound-speed measurements and could be subjected, in the future, to various and significant improvements.

To accomplish a first preliminary test of sound-speed measurements, water has been chosen due to the great amount of accurate literature data and its direct availability. After the microwave measurements under vacuum ($P_0 \cong 0$) had been carried out, antennae were dismounted and, without any other modification, the cell was placed in the high pressure vessel and thermostatted at $T_0 \cong 325\,\mathrm{K}$. The vessel was filled with purified

water, pressurized at 90 MPa, and pulse-echo measurements were made at 11 pressure points regularly spaced between 0.1 and 90 MPa. The variation of ΔL with pressure was calculated as $\Delta\mathrm{L}\ (T_0, \mathrm{P}) = \Delta\mathrm{L}\ (T_0, P_0)[1 - (\beta/3)\Delta\mathrm{P}]$ where β is the coefficient of adiabatic compressibility, which was calculated from published values [10] of the elastic constants of stainless steel. The relative magnitude of the correction required for the path length was 0.02% at the maximum pressure.

The pulse-echo measurement is based on a double reflector method. The piezoelectric disk, which separates the two microwave cylindrical cavities during dimensional measurements, is used as an ultrasonic pulse source at its thickness mode resonance frequency fixed at 4.35 MHz. Repeated tone bursts are delivered by a function generator to the piezo disk, and echoes coming from the reflectors are sampled by a digital oscilloscope. The analysis of echoes is accomplished as explained in Ref. 4; from the combined results of the time and dimensional measurements, the speed of sound was finally obtained.

From an acoustical point of view, each cylindrical cavity, with the piston-like source placed at its base and occupying its entire cross section, behaves as a wave guide for acoustic wave propagation. A sound wave propagating along a tube interacts with the side wall and undergoes thermal and viscous losses, thus presenting a modified phase velocity, with respect to the free-field condition, satisfying the relation

$$u = u_* \left[1 + \left(\frac{u_*}{\omega}\right)\alpha_{\mathrm{KH}}\right], \tag{6}$$

where u is the free-field phase velocity, u_* is the guided-wave phase velocity, ω is the angular frequency, and α_{KH} is the Kirchhoff–Helmholtz absorption coefficient, which depends on the transport properties of the medium:

$$\alpha_{\mathrm{KH}} = \frac{\omega}{2ub}\left[\delta_{\mathrm{sv}} + (\gamma - 1)\delta_{\mathrm{th}}\right], \tag{7}$$

$$\delta_{\mathrm{th}} = \sqrt{\frac{2\kappa}{\rho c_{\mathrm{P}}\omega}}, \tag{8}$$

$$\delta_{\mathrm{sv}} = \sqrt{\frac{2\eta}{\rho\omega}}, \tag{9}$$

(b is the radius of the circular tube, κ is the thermal conductivity, η is the viscosity, ρ is the density of the fluid, and c_{P} and c_{V} are the specific heat capacities at constant pressure and constant volume, respectively,

$\gamma = c_P/c_V$). This analysis, if applied to our experimental configuration, gives a correction on the order of 5 ppm.

Dispersion effects, on the other hand, could have non-negligible influence on the acoustic time-of-flight determination [11]. The carrier frequency of the acoustic pulses, being well above the cut-off frequency of the wave guide (which for the present experimental setup, is about 45 kHz), is compatible with the transmission of other modes different from the longitudinal plane wave. Those higher modes have phase velocities (greater than the sound speed in free space) which depend on the frequency of the signal,

$$u_{\text{phase}} = \frac{u}{\sqrt{1-(u\chi_n/\omega)}}, \tag{10}$$

where ω is the angular frequency of the signal, u is the sound speed in free field, and χ_n is a numerical constant depending on the symmetry of the mode and on boundary conditions. The corresponding group velocities, the only quantities accessible by experiment, are lower than the free field speed

$$u_g = u\sqrt{1-(u\chi_n/\omega)} = \left(\frac{u}{u_{\text{phase}}}\right)u. \tag{11}$$

If these non-longitudinal modes were excited by the source, the shape of acoustic pulses would be distorted by dispersion and the measured sound-speed would not coincide with the thermodynamic sound speed. The exhaustive theoretical work by Del Grosso [12] includes a model of dispersion and diffraction effects, which explains both pulsing and continuous wave acoustic propagation within cylindrical cavities. According to this model, if the quantity $z\lambda/a^2$ (where z is the acoustic path, λ is the wavelength, and a is the source radius) is much less than unity, the correction to the phase velocity coincides with that predicted for free-field diffraction. The model described in Ref. 13 allows calculations of a free-field diffraction correction, which in our case ($z\lambda/a^2 = 0.095; a \equiv b$, the inner diameter of the cylindrical cavities) is about 20 ppm.

4. PRELIMINARY RESULTS AND CONCLUSIONS

Data from pulse-echo acoustic measurements, in the form of time-of-flight determinations, have been combined with microwave dimensional measurements for a single isotherm at 325 K. The overall uncertainty of the present speed of sound measurements, estimated according to the procedure described in Ref. 4, is about 0.06%. Present data are compared with those available from other sources at 325 K [14, 15] and displayed as deviations from the IAPWS-95 formulation in Fig. 5. From

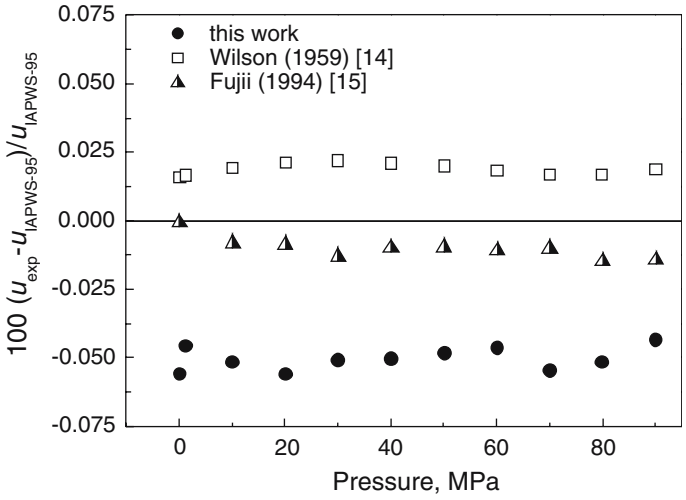

Fig. 5. Relative deviations of present data and other sources [14, 15] from IAPWS-95 formulation.

this comparison it is apparent that, while being affected by a low random noise, the present data show a systematic deviation from other sources that remains fairly constant as a function of pressure. The same systematic deviation is shown in Table II by a comparison with several accurate measurements at atmospheric pressure [16–19]. We attribute the lack of accuracy of present data to imperfect coupling of probes and resonant cavities during microwave measurements and the imperfect acoustic performance of the ultrasonic cell. A possible solution to the first problem could be a reduction of the length of the probes and recording and analysis of the reflected scattering coefficients. The second problem could be due to the poor efficiency of the 4 mm thick reflectors (ultrasonic pulses propagate

Table II. Comparison of Present Data and Other Sources for Speed of Sound in Pure Water $u_0 = u$ ($T = 325.00$ K, $p = 0.102325$ MPa)

Source	u_0 ($m \cdot s^{-1}$)	Uncertainty ($m \cdot s^{-1}$)
This work	1543.69	±0.78
Fujii and Masui [16]	1544.492	±0.015
Del Grosso and Mader [17]	1544.486	±0.015
Greenspan and Tschiegg [18]	1544.802	±0.046
McSkimin [19]	1544.46	±0.09

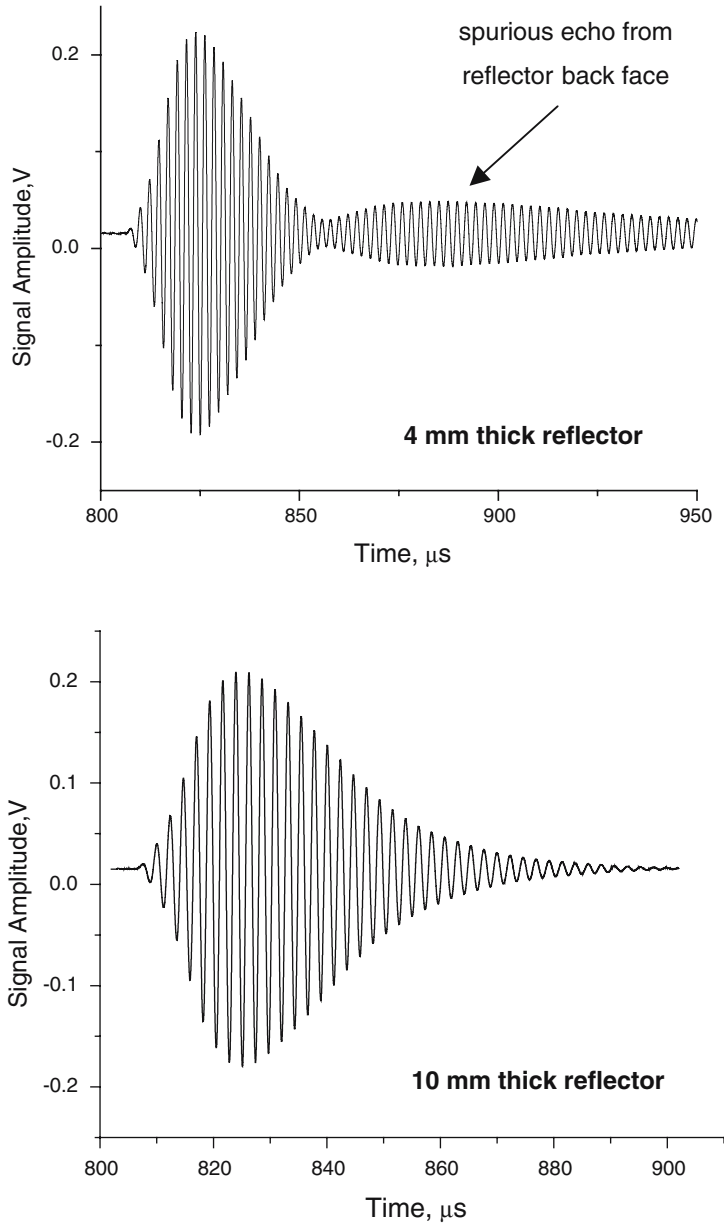

Fig. 6. Comparison of characteristic shape of acoustic echoes from different type of reflectors.

in the solid medium and are back-reflected by the outer surface towards the piezoelectric disk, interfering with the main acoustic echoes). To minimize this effect, which is shown in Fig. 6, the back surface of the reflectors should be reshaped to enhance their sound adsorption and dispersion characteristics.

REFERENCES

1. P. J. Kortbeek, M. J. P. Muringer, N. J. Trappeniers, and S. N. Biswas, *Rev. Sci. Instrum.* **56**:1269 (1985).
2. S. J. Ball and J. P. M. Trusler, *Int. J. Thermophys.* **22**:427 (2001).
3. W. Wagner and A. Pruss, *J. Phys. Chem. Ref. Data* **31**:387 (2002).
4. G. Benedetto, R. M. Gavioso, P. A. Giuliano Albo, S. Lago, D. Madonna Ripa, and R. Spagnolo, "Speed of Sound of Pure Water at Temperatures between 274 and 394 K and Pressures up to 90 MPa," paper presented at the 15th Symp. Thermophys. Props., Boulder, Colorado (2003).
5. W. J. Radcliffe and J. C. Gallop, *J. Phys. E: Sci. Instrum.* **14**:461 (1981).
6. M. B. Ewing and D. D. Royal, *J. Chem.Thermodyn.* **34**:1073 (2002).
7. M. R. Moldover, S. J. Boyes, C. W. Meyer, and A. R. H. Goodwin, *J. Res. Natl. Inst. Stand. Technol.* **104**:11 (1999).
8. C. J. Montgomery, in *Technique of Microwave Measurements* (McGraw-Hill, New York and London, 1947), pp. 300–302.
9. A. F. Clark, G. E. Childs, and G. H. Wallace, in *Adv. Cryo. Eng.*, Vol. 15, K. D. Timmerhaus, ed. (Plenum Press, New York and London, 1970), pp. 85–90.
10. ASM International Handbook Commiteee, J. R. Davis, ed., in *ASM Specialty Handbook – Stainless Steels* (ASM International, Materials Park, Ohio, 1994).
11. P. M. Morse and K. U. Ingard, in *Theoretical Acoustics* (Princeton University Press, Princeton, New Jersey, 1986), pp. 492–501.
12. V. A. Del Grosso, *Acustica* **24**:300 (1971).
13. R. Bass, *J. Acoust. Soc. Am.* **30**:602 (1958).
14. W. D. Wilson, *J. Acoust. Soc. Am.* **31**:1067 (1959).
15. K. Fujii, "Accurate Measurements of the Sound Velocity in Pure Water under High Pressure," paper presented at the 12th Symp. on Thermophys. Props., Boulder, Colorado (1994) and succeeding private communications.
16. K. Fujii and R. Masui, *J. Acoust. Soc. Am.* **93**:276 (1993).
17. V. A. Del Grosso and C. W. Mader, *J. Acoust. Soc. Am.* **52**:1442 (1972).
18. M. Greenspan and C. E. Tschiegg, *J. Res. Natl. Bur. Stand.* **59**:249 (1957).
19. H. J. McSkimin, *J. Acoust. Soc. Am.* **37**:325 (1965).